09 Jul 2012

Effect of Shock Front Geometry on Shock Depolarization of Pb(Zr 0.52Ti 0.48)O_3 Ferroelectric Ceramics

S. I. Shkuratov

Jason Baird
Missouri University of Science and Technology, jbaird@mst.edu

E. F. Talantsev

Effect of shock front geometry on shock depolarization of $Pb(Zr_{0.52}Ti_{0.48})O_3$ ferroelectric ceramics

Sergey I. Shkuratov,[1,a)] Jason Baird,[1,2] and Evgueni F. Talantsev[3]
[1]*Loki Incorporated, Rolla, Missouri 65409, USA*
[2]*Department of Mining and Nuclear Engineering, Missouri University of Science and Technology, Rolla, Missouri 65409-0450, USA*
[3]*Pulsed Power LLC, Lubbock, Texas 79416, USA*

(Received 3 May 2012; accepted 15 June 2012; published online 9 July 2012)

By use of experimentation, we detected a shock wave geometry effect on the depolarization of poled $Pb(Zr_{0.52}Ti_{0.48})O_3$ (PZT 52/48) ferroelectrics. It follows from the experimental results that shock front geometry is one of key parameters in the shock depolarization of PZT 52/48 ferroelectrics. This shock depolarization effect forms a fundamental limit to miniaturization of explosive-driven shock-wave ferroelectric generators (FEGs). Based on obtained experimental results, we developed miniature generators that reliably produce pulsed voltages exceeding 140 kV. © *2012 American Institute of Physics*. [http://dx.doi.org/10.1063/1.4732809]

I. INTRODUCTION

Over the past five decades, planar impact methods and velocity interferometry diagnostics have been used extensively to provide high-resolution shock-profile data for ceramic materials[1] including ferroelectric ceramics.[2,3] The advantages of a planar shock wave (stable geometry, constant pressure along the front, constant shock wave front velocity) made it possible to simplify the theoretical models used for the analysis of these shock wave experiments.[1] One of the effects associated with shock-wave compression of ceramic materials is shock depolarization of poled ferroelectrics.[4] Since the 1960s, it has been well established that the shock front pressure is a key parameter in the shock depolarization of poled ferroelectrics. The shock depolarization effect is utilized for development of miniature autonomous prime power sources that are in demand in some modern scientific and engineering projects.[5] The sizes of experimental systems used for investigation of materials compressed by planar shock waves are typically very large,[1,6] and these techniques cannot be used to initiate a shock wave in miniature ferroelectric generators.

Earlier we reported on the depolarization of poled $Pb(Zr_{0.52}Ti_{0.48})O_3$ ceramic elements within compact FEGs utilizing a nearly planar shock wave initiated by an explosively-accelerated metallic impactor (flyer plate).[7,8] These longitudinal and transverse (shock wave propagates along and across the polarization vector $\boldsymbol{P}_0$, correspondingly) FEGs routinely produce output voltages exceeding 45 kV.[7–10] However, the presence of a flyer plate significantly increases the amount of high explosives (HE) required, increases the size and weight of the generators, and becomes a limiting factor for further miniaturization of power sources.

Recently we reported on the development of a series of compact sources of prime power utilizing transverse shock depolarization of PZT 52/48 ferroelectric ceramic elements by nearly planar shock waves initiated directly from the HE charge.[11] The developed FEG design[11] can be used as a basis for further miniaturization of ferroelectric prime power sources in order to create autonomous high-voltage and high-current generators with less than 15 cm^3 in total volume. Scaling down the size of FEGs and, correspondingly, the size of HE charges raises a fundamental question – what will the effect be on shock depolarization of ferroelectrics and their ability to produce prime power? To answer this question we have studied ferroelectric materials compressed by shock waves generated by the detonation of miniature HE charges. The results are reported in this paper.

II. MATERIALS AND EXPERIMENTAL TECHNIQUES

A schematic diagram of the experimental device we used is in Fig. 1. The FEG contained two parts (Fig. 1): a detonation chamber and a ferroelectric element encapsulated within the plastic body by epoxy; there were no moving metallic parts. The shock wave in the PZT 52/48 element was generated by coupling the HE detonation shock through direct contact with the epoxy potting material and into the ferroelectric element. We used desensitized RDX and RISI RP-501 detonators for the explosive charges. Explosive experiments were conducted in the facilities of the Energetic Materials Research Laboratory of the Missouri University of Science and Technology, Rolla, MO. Other experimental details are described elsewhere.[7–12]

Rectangular PZT 52/48 (EC-64) ceramic elements, 12.7-mm thick × 12.7-mm wide × 50.8-mm long were supplied by ITT Corporation for these experiments. The ferroelectric elements were poled across their thickness dimension by the manufacturer. The physical properties of the PZT 52/48 (EC-64) are: density $7.5 \cdot 10^3$ kg/m^3, dielectric constant $\varepsilon = 1300$, Curie temperature 320°C, Young's modulus $7.8 \cdot 10^{10}$ N/m^2, piezoelectric constant $d_{33} = 295 \cdot 10^{-12}$ C/N.

a)E-mail: shkuratov@lokiconsult.com.

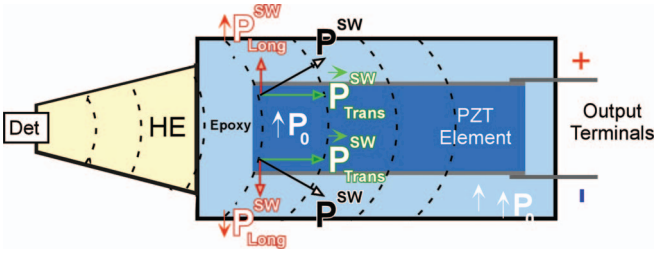

FIG. 1. Schematics of the shock-wave ferroelectric generator. $\boldsymbol{P}^{SW}$ is the shock compression vector. $\overrightarrow{P_{long}^{sw}}$ and $\overrightarrow{P_{trans}^{sw}}$ are longitudinal and transverse components of the shock compression vector, correspondingly. $\boldsymbol{P}_0$ is the polarization vector.

III. RESULTS AND DISCUSSIONS

The operation of an FEG (Fig. 1) was as follows. After initiation of the detonator, the detonation wave propagated in the HE charge toward to the top of the epoxy/plastic body. The shock wave front transmitted through the epoxy reached the PZT 52/48 element and propagated through it. Because of shock depolarization, the electric charge contained within the poled ferroelectric element was released at the element electrodes and a pulsed electromotive force (e.m.f.) appeared at the output terminals of the FEG. The amplitude of the e.m.f. pulse generated at the electrodes of the elements depended on the degree of the shock depolarization.

To study the effect of HE-charge size and geometry on the degree of shock depolarization of ferroelectric element we designed four types of ferroelectric generators (see the four cases in Table I) differed in the HE mass and HE charge output diameter. Because the shock wave in the ferroelectric element originated from the detonating HE charge (Fig. 1), the shock wave parameters affecting the ferroelectric element were determined by the geometry of the HE chamber, the explosive type, parameters, initiation point, the geometry of the plastic FEG body, and by the shock impedance matching among the explosive, the explosive chamber, epoxy potting, plastic FEG body, and the ferroelectric element. The geometrical dimensions and masses of explosives for investigated cases are in Table I. Note that a truncated cone of hand-packed desensitized RDX was the explosive charge used in each case.

Typical e.m.f. waveforms, $U_g(t)$, produced in the cases are in Fig. 2. Table I summarizes the experimental results for all four cases. It follows from the experimental data that a two-fold increase of the mass of HE (Cases 1 and 2) did not result in an increase of the amplitude of the e.m.f. produced by the shocked PZT 52/48 element. An increase of the charge

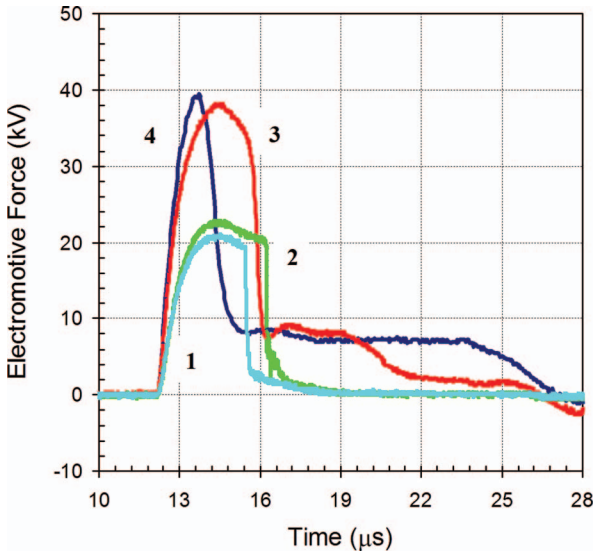

FIG. 2. Typical e.m.f. waveforms produced by FEGs operating with a 12.7 mm × 12.7 mm × 50.8 mm PZT 52/48 element for Case 1 (Plot 1), Case 2 (Plot 2), Case 3 (Plot 3), and Case 4 (Plot 4).

output diameter from 19 mm (Case 2) to 32 mm (Case 3) resulted in a significant increase of the e.m.f. amplitude even though the HE mass was reduced. However, nearly doubling the charge output diameter from 32 mm to 56 mm made little change in U_g (Case 4).

It follows from the experimental results (Fig. 2 and Table I) that it is possible to generate an e.m.f. pulse with almost twice the amplitude with no change in the PZT 52/48 element size and a decrease in the explosive mass. It is important to understand the nature of this effect.

In all theoretical models (extended list of references can be founded in Ref. 5), the shock pressure magnitude, $|\overrightarrow{P^{sw}}|$, is a key parameter in the shock depolarization of poled ferroelectrics.[3] Regarding this pressure, once certain critical minimum values of mass and density are achieved, the detonation steady-state condition depends primarily on the explosive charge geometry.[13] The minimum charge length to create the greatest impulse at the end of the charge opposite the detonator is approximately three times the effective charge diameter for a confined cylindrical charge,[13] but our charges were confined truncated cones. We made a reasonable assumption, later borne-out in our experiments, that we could consider the smaller base of the right circular cone frustum (the detonator location) as the charge diameter (7 mm) to determine the minimum effective charge length. As such, the minimum effective charge length was approximately 22 mm (see Table I).

TABLE I. Geometry of the truncated cone RDX HE charge, its mass, radius of shock front at the first contact with PZT sample, the amplitude of e.m.f. pulse produced by shock-compressed $Pb(Zr_{0.52}Ti_{0.48})O_3$ element of 12.7 × 12.7 × 50.8 mm^3 dimensions, and longitudinal and transverse shock compression components at the edges of the ferroelectric sample.

Case designation	HE charge length, (mm)	HE mass, (g)	HE charge/epoxy interface diameter, (mm)	e.m.f. amplitude U_g, (kV)	HE charge cone angle, (degree)	Shock front radius, R (mm)	$\frac{\lvert\overrightarrow{P_{long}^{sw}}\rvert}{\lvert\overrightarrow{P^{sw}}\rvert}$	$\frac{\lvert\overrightarrow{P_{trans}^{sw}}\rvert}{\lvert\overrightarrow{P^{sw}}\rvert}$
Case 1	34	9.3 ± 0.7	19	21.1 ± 1.1	12	35	0.26	0.97
Case 2	42	18.3 ± 0.5	19	21.9 ± 1.3	4	35	0.26	0.97
Case 3	22	10.4 ± 0.7	32	38.7 ± 1.2	60	60	0.15	0.99
Case 4	45	59.0 ± 2.5	56	38.9 ± 1.3	60	60	0.15	0.99

At the explosive-epoxy interface, the desensitized RDX used in Case 1 and 2 should have achieved at least 22.4 GPa detonation (Chapman-Jouguet) pressure at a density of 1.58 g/cm^3, a reasonable density for hand-packing this type of explosive, given an explosive mass of greater than 0.5 g and a volume of at least 1 cm^3 (details are given in Ref. 13). This pressure, 22.4 GPa, is significantly higher than that determined to be necessary for the shock depolarization of PZT 52/48 ferroelectrics.[3] Therefore, different shock pressures in the investigated cases cannot explain the decreased e.m.f. pulse amplitude.

A possible explanation of the observed shock depolarization effects relates to shock wave geometry. The shock waves generated in the ferroelectric elements (Fig. 1) did not have planar geometry, but had hemispherical geometry. For charge lengths at and beyond the minimum effective charge length, the radius of curvature of the front of the detonation head within the explosive is effectively constant no matter the charge diameter. The ratio of the limiting radius of curvature to the charge diameter is approximately 3.5 for RDX in this case (a charge length equal to or greater than the minimum effective charge length).[13,14] Therefore, as long as the charge length equals or exceeds the minimum effective charge length, the radius of curvature of the shock, R, will be the same at the explosive-to-epoxy interface, whatever the actual length of the charge. The radius of curvature of the shock front at the end of the PZT element as calculated for each case is in Table I.

The non-planar geometry of the shock front (Fig. 1) resulted in dividing the shock wave compression vector, $\overrightarrow{P^{sw}}$, affecting the ferroelectric sample into two parts: transverse, $\overrightarrow{P^{sw}_{trans}}$, and longitudinal, $\overrightarrow{P^{sw}_{long}}$ (across and along the polarization vector, $\boldsymbol{P}_0$, correspondingly). Shock compression vectors $\overrightarrow{P^{sw}_{long}}$ and $\overrightarrow{P^{sw}_{trans}}$ are shown in Fig. 1. The magnitude of longitudinal part of shock compression vector in each point within the shocked ferroelectric sample is inversely proportional to the radius of the curvature of the shock front, R,

$$\left|\overrightarrow{P^{sw}_{long}}\right| = \left|\overrightarrow{P^{sw}}\right| \cdot |\sin(\phi)| = \left|\overrightarrow{P^{sw}}\right| \cdot \frac{h}{R}, \tag{1}$$

where, h is the distance between a given point and centerline of the PZT sample, and ϕ is the angle between the shock vector direction and the vector component in question. The magnitude of the transverse component can be calculated as follows:

$$\left|\overrightarrow{P^{sw}_{trans}}\right| = \left|\overrightarrow{P^{sw}}\right| \cdot |\cos(\phi)| = \left|\overrightarrow{P^{sw}}\right| \cdot \left(1 - \left(\frac{h}{R}\right)^2\right)^{\frac{1}{2}}. \tag{2}$$

Values for $\frac{|\overrightarrow{P^{sw}_{long}}|}{|\overrightarrow{P^{sw}}|}$ and $\frac{|\overrightarrow{P^{sw}_{trans}}|}{|\overrightarrow{P^{sw}}|}$ calculated for the PZT sample edges are given in Table I. It follows from the calculations that the transverse component of shock compression stays practically the same for all cases, but the longitudinal component, $\frac{|\overrightarrow{P^{sw}_{long}}|}{|\overrightarrow{P^{sw}}|}$, changes significantly (it increases from 0.15 in Case 3 to 0.26 in Case 2). The significant change of the longitudinal component of shock compression makes it possible to propose an explanation for the observed decrease in e.m.f. pulse amplitude (Fig. 2 and Table I). Earlier,[2,3] Reynolds and Seay showed that a longitudinal shock wave in PZT 52/48 splits into two shock waves. The split shocks result in a decreased depolarization charge. Recently,[9] we experimentally demonstrated that such shock splitting leads to a significant decrease in e.m.f. pulse amplitudes generated by longitudinal-shock-compressed PZT 52/48 samples with thicknesses exceeding 6.5 mm. Apparently, shock splitting creates significant problems in the depolarization of the 12.7 mm-thick PZT 52/48 samples investigated in this paper.

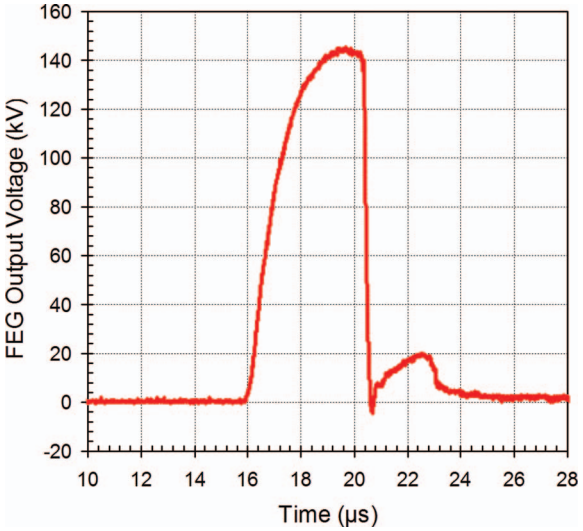

FIG. 3. Typical waveform of e.m.f. pulse produced by an FEG containing a 63.5 mm × 12.7 mm × 50.8 mm PZT 52/48 element.

The PZT samples were subjected to both transverse and longitudinal shock depolarization, and therefore the part of the shock depolarization charge related to the longitudinal component may have been lost due to the shock splitting phenomena. When the radius of the shock front was reduced to $R = 35$ mm (see Table I), a larger part of shock wave energy was involved in longitudinal shock compression of the PZT 52/48 sample. This resulted in an intensification of the shock splitting process and in greater depolarization charge losses.

To explore development of real world miniature devices based on the shock depolarization effects described above, we designed and tested a series of miniature ultra-high voltage FEGs with diameters of 40 mm, 50 mm and 63 mm. These miniature generators (each with a volume less than 180 cm^3) were capable of producing output voltages exceeding 100 kV. A typical waveform of the e.m.f. pulse produced by one of these generators is in Fig. 3. The total thickness of the PZT 52/48 element was 63.5 mm. The amplitude of the e.m.f. was 143 kV with $\tau = 2.5$ μs, and a pulse duration of 10 μs.

IV. CONCLUSIONS

We experimentally demonstrated that shock front geometry is one of the key parameters in the shock depolarization of poled $Pb(Zr_{0.52}Ti_{0.48})O_3$ ferroelectrics. This shock

depolarization effect should be considered as one of the fundamental limits to miniaturization of shock-wave ferroelectric generators. Miniature prime power sources designed with an understanding of the herein described shock depolarization effect are capable of producing output voltage pulses with amplitudes exceeding 140 kV. These generators are available for use as sources of prime power in new scientific and engineering applications.[5,15]

[1]D. E. Graddy, Mech. Mater. **29**, 181 (1998).
[2]C. E. Reynolds and G. E. Seay, J. Appl. Phys **32**, 1401 (1961).
[3]C. E. Reynolds and G. E. Seay, J. Appl. Phys. **33**, 2234 (1962).
[4]F. W. Neilson, Bull. Am. Phys. Soc. **2**, 302 (1957).
[5]L. L. Altgilbers, J. Baird, B. Freeman, C. S. Lynch, and S. I. Shkuratov, *Explosive Pulsed Power* (Imperial College Press, London, U.K., 2011).
[6]S. M. Walley, Adv. Appl. Ceramics **109**, 446 (2010).
[7]S. I. Shkuratov, E. F. Talantsev, L. Menon, H. Temkin, J. Baird, and L. L. Altgilbers, Rev. Sci. Instrum. **75**, 2766 (2004).
[8]S. I. Shkuratov, J. Baird, V. G. Antipov, E. F. Talantsev, C. Lynch, and L. L. Altgilbers, IEEE Trans. Plasma Sci. **38**, 1856 (2010).
[9]S. I. Shkuratov, J. Baird, and E. F. Talantsev, Rev. Sci. Instrum. **81**, 126102 (2010).
[10]S. I. Shkuratov, E. F. Talantsev, and J. Baird, J. Appl. Phys. **110**, 024113 (2011).
[11]S. I. Shkuratov, J. Baird, and E. F. Talantsev, Rev. Sci. Instrum. **82**, 086107 (2011).
[12]S. I. Shkuratov, J. Baird, and E. F. Talantsev, Rev. Sci. Instrum. **82**, 054701 (2011).
[13]M. W. Cook, *The Science of High Explosives* (American Chemical Society/Robert E. Krieger, Huntingtion, NY, 1971).
[14]J. Baird, Ph.D. Dissertation, University of Missouri, Rolla, 2001.
[15]J. Baird and S. Shkuratov, Loki Incorporated, U.S. patent 7,560,855 (14 July 2009).